Heliyon 8 (2022) e09769

Contents lists available at ScienceDirect

Heliyon

journal homepage: www.cell.com/heliyon

Research article

Positive effects of Phycocyanobilin on gene expression in glutamate-induced excitotoxicity in SH-SY5Y cells and animal models of multiple sclerosis and cerebral ischemia

Daniel Palenzuela Gardón [a,e,1], Majel Cervantes-Llanos [a,1], Beatriz Piniella Matamoros [a], Hanlet Camacho Rodríguez [a], Chan-yuan Tan [e], Javier Marín –Prida [b], Viviana Falcón-Cama [a,f], Nancy Pavón-Fuentes [c], Jessica Gómez Lemus [d], Laura de la Caridad Bakos Ruiz [a], Tamara Díaz Argudin [a], Gillian Martínez Donato [a,e], Yasser Perera [a,e], Ke Yang [e,**], Giselle Pentón-Rol [a,f,*]

[a] Center for Genetic Engineering and Biotechnology (CIGB), Ave. 31 e/ 158 y 190, Cubanacán, Playa, Havana, PO Box 6162, Cuba
[b] Center for Research and Biological Evaluations, Institute of Pharmacy and Food, University of Havana, Ave. 23 e/ 214 y 222, La Lisa. PO Box: 430, Havana, Cuba
[c] International Center for Neurological Restoration (CIREN), Havana, Cuba
[d] Faculty of Biology, University of Havana, Havana, Cuba
[e] China-Cuba Biotechnology Joint Innovation Center (CCBJIC), Yongzhou Zhong Gu Biotechnology Co., Ltd, Yangjiaqiao Street, Lengshuitan District, Yongzhou City 425000, Hunan Province, China
[f] Latin American School of Medicine, Calle Panamericana Km 3 1/2, Playa, Havana, 11600, Cuba

ARTICLE INFO

Keywords:
Phycocyanobilin
qPCR
PCA
Glutamate
Oxidative stress
Multiple sclerosis
Cerebral ischemia

ABSTRACT

Background: Oxidative stress has a predominant role in the pathogenesis of neurodegenerative diseases and therefore the modulation of genes and the identification of biological pathways associated with antioxidant therapies, have an impact on its treatment.
Objective: The objective of this study was the comparison of 2 methods for the analysis of real-time PCR (qPCR) data, through the use of the evaluation of genes that mediate the effect of Phycocyanobilin (PCB) and its validation in animal models.
Methods: We evaluated the effect of PCB:" in vitro" on gene modulation through qPCR analyzed by parametric ANOVA and multivariate principal component analysis (PCA) in a model of glutamate-induced excitotoxicity in the SH-SY5Y cell line and" in vivo"; in animal models of multiple sclerosis (MS) and cerebral ischemia (CI).
Results: The results showed that PCA is a robust and powerful method that allows the assessment of gene expression profiles. We detected the significant down-regulation of the *CYBB* (NOX2), and HMOX1 by the action of PCB in SH-5YSH cell line insulted with Glutamate. The decrease in pro-inflammatory cytokines and markers related to apoptosis and innate immune response, mediated the effect of PCB in the animal models of MS and CI, respectively.
Conclusion: We concluded that the mechanisms by which PCB protected cells included the reduction of oxidative stress damage, which could contribute to its clinical efficacy for the treatment of neurodegenerative diseases.

1. Introduction

Differentially expressed genes (DEGs) are a tool used in drug development and in the study of the mechanism of action of drugs, since identifying the set of modified target genes allows knowing the pathways by which our drug exerts its effect (Chengalvala et al., 2007). The purpose of DEG analysis is often to contrast gene pattern expression modifications in diseased individuals with apparently healthy controls and/or

* Corresponding author.
** Corresponding author.
E-mail addresses: young@ccbjic.com (K. Yang), giselle.penton@cigb.edu.cu (G. Pentón-Rol).
[1] These authors contributed equally to this study and should be considered as co-first authors.

https://doi.org/10.1016/j.heliyon.2022.e09769
Received 8 October 2021; Received in revised form 11 November 2021; Accepted 16 June 2022

those receiving therapy. Alterations in gene expression may be interpreted as the modification of a particular pathway, leading to disease progression and in turn affecting response to drugs (Rodriguez-Esteban and Jiang, 2017). In this sense, a promising drug candidate for different neurodegenerative diseases has been reported in recent years, named Phycocyanobilin (PCB) (Pentón-Rol et al. 2021), for which the identification of the DEGs involved in its pharmacological actions may pave the way to better understand its modes of actions. PCB is an open-chain tetrapyrrole chromophore covalently bonded to both polypeptide chains of C-Phycocyanin (C-PC), the most represented biliprotein of *Spirulina platensis* (Padyana et al., 2001). PCB exhibits several biological effects including antioxidant and anti-inflammatory, in addition to immunomodulatory capacity (Fernández-Rojas et al., 2014). It is, therefore, suspected that DEGs may be involved in these specific PCB activities in cells, in particular, the redox pathways (Radi, 2018).

Aerobic organisms continuously produce ROS as metabolic intermediates of cellular respiration. They encompass anion superoxide (O2•) and hydroxyl (•OH) radicals, also non-radical species like hydrogen peroxide (H_2O_2) (Bae et al., 2011). Oxidative stress appears as a consequence of the ROS formation exceeding the antioxidant capacity of the cell and/or the malfunctioning of the antioxidant defenses system (Martindale and Holbrook, 2002). Oxidative modifications of these macromolecules mediate the development of several pathologies. Neurodegenerative diseases are morphologically featured by progressive cell loss in specific vulnerable neuronal cells, often associated with cytoskeletal protein aggregates forming inclusions in neurons and/or glial cells (X. Chen, Guo, and Kong, 2012).

This study aimed to characterize the effects of PCB on the gene expression in the SH-SY5Y cell line derived from human neuroblastoma tissue (Xie et al. 2010). The expression profile induced by PCB was compared to Control cells (not treated) and treated with Glutamate. The excitotoxicity produced by glutamate in neuroblastoma SH-SY5Y cells is most likely triggered by oxidative stress according to the results of Sun et al. who also report a decrease in antioxidant defenses such as glutathione content and the enzyme superoxide dismutase (SOD) and elevation of extracellular levels of malonyl dialdehyde (MDA) (Sun et al., 2010). For this work, we used real-time PCR (qPCR) considered to be one most effective methods to analyze modulations in gene expression because of its efficiency to detect and precisely quantify the target genes, even at low expression levels (Lech and Anders, 2014). In the analysis of qPCR data, two methods were used: parametric ANOVA and multivariate principal component analysis (PCA). This technique was used to evaluate the effect of PCB on the modulation of genes related to oxidative stress, inflammation, and hypoxia. Furthermore, in this study, the validation of the effect of PCB was carried out with the use of animal models of Multiple Sclerosis (MS) and cerebral ischemia (CI), in which these processes play a determining role in their pathogenesis.

2. Materials and methods

2.1. Reagents

All chemicals used were of the highest grade available and purchased from Sigma-Aldrich (St. Louis, MO, USA) unless otherwise specified. PCB was obtained from Santa Cruz Biotechnology (Cat. No. SC-396921).

2.2. Cell culture and experimental groups

Human SH-SY5Y cells were maintained in culture DMEM/F12 medium supplemented with fetal bovine serum, penicillin, streptomycin, and L-glutamine. The cells were divided into 4 groups, each one containing approximately 4 million SH-SY5Y cells: (**1**) Non-treated cells (used as a control), (**2**) PBC, (**3**) PBC plus Glutamate, and (**4**) Glutamate (See table below)

After 24 h of pre-stimulation with PCB (0.1uM) (groups 2 and 3), media was replaced with freshly prepared PCB (0.01uM) (group 2) and PBC (0.01uM) plus Glutamate (60uM) (group 3) and Glutamate alone (60uM) (group 4) for another day. All groups were incubated for the next 4 h.

	Group 1 (Control)	Group 2	Group 3	Group 4
0–24h	DMEM/F12 fully suppl medium	DMEM/F12 fully suppl medium + PCB (0.1uM)	DMEM/F12 fully suppl medium + PCB (0.1uM)	DMEM/F12 fully suppl medium
24h-	- DMEM/F12 fully suppl medium	DMEM/F12 fully suppl medium + PCB (0.01uM)	DMEM/F12 fully suppl medium + PCB (0.01uM) + Glutamate (60uM/40uM)	Glutamate (60uM/40uM)
Endpoint	+4 h qPCR	+4 h qPCR	+4 h qPCR	+4 h qPCR

Afterward, the medium was removed; cells were washed using cold PBS and processed to conduct gene expression analysis. Three biological replicates were taken per group.

2.3. RNA extraction and quality (S.1.1 Suppl)

To stabilize total RNA, the cells were centrifuged and suspended in 1 mL of RNA later (Qiagen). Samples were homogenized and total RNA was isolated using the miRNeasy Mini Kit (Qiagen, Hilden, Germany), including small RNAs fraction from approximately 18 nucleotides (nt) upwards. Total RNAs were quantified using a Qubit™ RNA HS Assay Kit (Cat. Q32855, Thermo Fisher, USA) and the RNA integrity was analyzed by 2100 Bioanalyzer (Agilent RNA 6000 Nano Kit, Waldbronn, Germany); RNAs with a 260:280 ratio of $\geq$1.5 and an RNA integrity number of $\geq$6.5 were used in the study. Two replicates of each Total RNA sample were processed independently. In total 24 RNA samples were studied and distributed in 4 groups similar to the previous groups.

2.4. RT-qPCR and identification of optimal reference genes (RG) (S.1.2 Suppl)

The gene mRNA levels were measured by RT-qPCR based on LightCycler 480 SYBR Green I Master kit instructions, in the LightCycler480 II machine (Roche, Germany). Briefly, the reaction contained 10 μL of SYBR Green I Master. The concentration of each primer was previously optimized between 300 nM, 600 nM, and 900 nM. A volume of 4 μL cDNA was added to the 16 μL of PCR Mix. The total PCR reaction volume was 20 μL. The reactions were performed in duplicate. The PCR cycler conditions were the same for all transcripts: 95 °C for 5 min, 40 cycles at 95 °C for 5 s, and a combined annealing and extension step at 60 °C for 10 s. We also used the ValidPrime® Control for Genomic Background kit (Cat. A105S10, TataaBiocenter, Sweeden) to estimate and correct for gDNA contribution in RT (+)–qPCR measurements in a more reliable manner than that afforded by RT (-) controls (Henrik and Iacovoni, 2012).

2.5. Gene selection and primers design

The genes were selected based on our past research and literature on the topic. We took into account key genes involved in the next pathways: oxidative stress and antioxidant defense, nitric oxide signaling, multiple sclerosis, apoptosis, and neurodegenerative diseases such as Alzheimer's disease, and multiple sclerosis (Table 1—Suppl). To select the genes the information available for PrimePCR Disease State Panels designed by referencing the National Library of Medicine database was considered ("PrimePCR Pathways" n.d.)

The primer sequences were designed considering an intron-spanning primer pair with a minimum intron length of 700 bp to avoid amplification of genomic DNA. Both software Primer 3 plus and Primer-Blast were used to design the primers. The primers were synthesized by Sangon Biotech (Shanghai, China) (Table 2—Suppl).

2.6. Relative quantification and statistical analysis

To perform the gene expression profile analysis, we used the Genex Enterprise software, which contains advanced data analyzes including Dynamic PCA, ROC curve, Artificial Neural Network, and Support Vector Machine. GenEx Enterprise also provides modules for data analysis conforming to the Clinical and Laboratory Standards Institute (CLSI) standard documents. Firstly, we performed the important preprocessing steps such as the handling of missing data, inter-plate calibration, gDNA background subtraction, gene reference, and mean-centered normalization. The relative expression of the target genes was calculated in comparison with the sample with a maximum Cq value. The normalized expression matrix was loaded into the Genex and the differences between groups were analyzed by one-way analysis of variance (ANOVA) followed by Turkey-Kramer's post hoc test to do all pairwise comparisons. Also, the R package Factominer was used to perform principal component analysis.

2.7. EAE induction in C57BL/6 mice and PCB treatment (S.1.3 Suppl) and measurement of cytokines by ELISA

Female C57BL/6 mice, 8–10 weeks old were obtained from the Animal Care Facilities of the Federal University of Minas Gerais, Belo Horizonte, Brazil. The animals were kept on a light/dark cycle of 12 h and were given food and water ad libitum. Procedures involving animals comply with national and international regulations and policies (EEC Council Directive 86/609, OJL 358, 1, 12 December 1987; Guide for the Care and Use of Laboratory Animals, US Nitti et al., 2018), and were approved by the institutional animal ethics committee of the Federal University of Minas Gerais, CNPq Nº 03/2014, Belo Horizonte, Brazil.

On day 28 post-immunization, mice were anesthetized with 40 mg/kg sodium pentobarbital (i.p) ("Anesthesia and Analgesia in Laboratory Animals - 2nd Edition" n.d.). Brains were dissected excluding olfactory bulbs and cerebellum. Both brain hemispheres were divided at the sagittal plane at 2.0 mm from the bregma. The region closest to the sagittal suture was used for the quantification of proinflammatory cytokines by ELISA. Shortly, 100 mg of tissue were homogenized using an Ultra-Turrax device (IKA Works, Inc., USA) in 1 mL of ice-cold extraction solution containing 0.4 M NaCl, 0.05% Tween 20, 0.5% bovine serum albumin, 0.1 mM phenylmethylsulfonylfluoride, 0.1 mM benzethonium chloride, 10 mM EDTA and 20 KIU aprotinin prepared in PBS. Supernatants were obtained by centrifugation at 15,000 $\times$g for 10 min at 4 °C and stored at −70 °C until use. The expression levels of IL-17, IL-6, and IFN-γ were quantified using the corresponding ELISA Kits (R&D Systems, Minneapolis, MN, USA). All procedures were performed according to the manufacturer's protocols.

2.8. Surgery procedure and treatment (S.1.4 Suppl) and transmission electron microscopy and immunodetection

Male Wistar rats (CENPALAB, Havana, Cuba) were maintained under standard laboratory conditions (60% humidity, 22 ± 1 °C, and 12 h light/darkness cycle) with free access to food and water. The procedures were approved by the institutional ethics committee of the International Center for Neurological Restoration- 05/2014, Havana, Cuba, in compliance with the European Community's Council Directive of November 24th 1986 (86/609/EEC) and the ARRIVE guidelines for animal experimentation.

One day after ET-1 injection, rats (n = 5 each group) were killed and brain tissue samples were fixed for 1 h at 4 °C in 1% (v/v) glutaraldehyde and 4% (v/v) paraformaldehyde, rinsed in 0.1 mol/L sodium cacodylate (pH 7.4), then post-fixed for 1 h at 4 °C in 1% OsO4, and dehydrated in increasing concentrations of ethanol. Ultrathin sections (400–500 Å) made with an ultramicrotome (NOVA, LKB) were placed on 400 mesh grids, stained with saturated uranyl acetate and lead citrate, and examined with a JEOL/JEM 2000 EX transmission electron microscope (JEOL) (Spurr, 1969). Ultrathin brain sections were incubated with the anti-caspase 3 and anti-CD11 (Abcam, Cambridge, UK) at a 1:10 dilution. After repetitive rinses, they were incubated for 1 h at room temperature with gold-labeled (15 nm) secondary anti-mouse IgG (Amersham, UK) diluted 1:50. As a control, the primary antibody was substituted by normal mouse serum. The expression density was determined with ImageJ 1.41 program (National Institutes of Health, Bethesda, MD, USA).

3. Results

3.1. Identification of most stable housekeeping genes and samples outliers

The most stable gene identified by Normfinder was *ACTB* with the maximum confounding variance due to random noise of 0.048 cycles, a value that is low considering that the confounding variance from the PCR instrument could be as high as 0.25 cycles. The intragroup standard deviation (STD) is shown for different treatments where all four assessed genes showed STD values below 0.25 cycles, and therefore all of them can be used in the analysis (Tab. 3- Suppl). In Fig. S1 Supp Normfinder STD value and geNorm M-values are shown for all studied genes. Normfinder identified *ACTB* and *TBT* as the most appropriate pair of RGs for normalization. Meanwhile, *ACTB* and *GAPDH* genes were identified by geNorm. Notably, normalization performed with the Normfinder pair of genes was able to detect more significant genes than geNorm.

On the other hand, data quality assessment and quality control are essential steps of any data analysis. The multidimensional scaling (MDS) plot is frequently used to explore differences in samples. The MDS analysis was done in R. Fig. S2 Suppl shows that the sample PG_2 was plotted apart from the rest of the samples' cluster (PG_1 and PG_3) and was considered to be an outlier, and hence, it was removed from the subsequent analysis.

3.2. Assessment of correlation between genes

Before performing the PCA analysis, we checked the correlation matrix for variables (Figure 1). The distribution of each variable is shown on the diagonal. On the bottom of the diagonal: the bivariate scatter plots with a fitted line are displayed. On the top of the diagonal: the value of the correlation plus the significance level as stars. We can see that *APP*, *BACE1*, *VEGFA*, and *NCF1* have a significant strong positive correlation. Meanwhile, *CYBB* and *IRP1* show a significant negative correlation with respect to previous variables.

3.3. Differentially expressed genes in SH-SY5Y cells subjected to high-level glutamate injury treated with PCB

The one-way ANOVA was used to evaluate any evidence of groups means difference using the preprocessed normalized matrix loaded into Genex. Genes *NCF*, *APP*, *BACE*, and *CYBB* showed a p-value below the cut-off (0.006) to control the type I error in multiple comparisons (Chen et al., 2017). *VEGF* and NOS had a border significance with a p-value below 0.05 but above the corrected p-value.

Figure 2 shows the relative gene expression and the Tukey-Kramer posthoc comparisons, which find which specific group's means are different. *CYBB* expression was significantly reduced in PCB + Glutamate group compared to the rest of the groups. Overall, we observed that incubation of SH-SY5Y cells with Glutamate combinations increased mRNA expression for *NOS*, *APP*, *BACE*, *VEGFA,* and *NCF*. Meanwhile, *CYBB* decreased mRNA expression after treatment with the combination of PCB + Glutamate. A downregulation of *CYBB* was the most relevant result, with the aim of identifying which of the modulated genes in this model could have a beneficial effect in knowing the effect of PCB in the glutamate-induced excitotoxicity model.

In the PCA the first dimensions account for most of the data inertia (variability) (Jolliffe and Jorge, 2016). In our case, the first two dimensions express 84.8% of the total dataset inertia; that means that

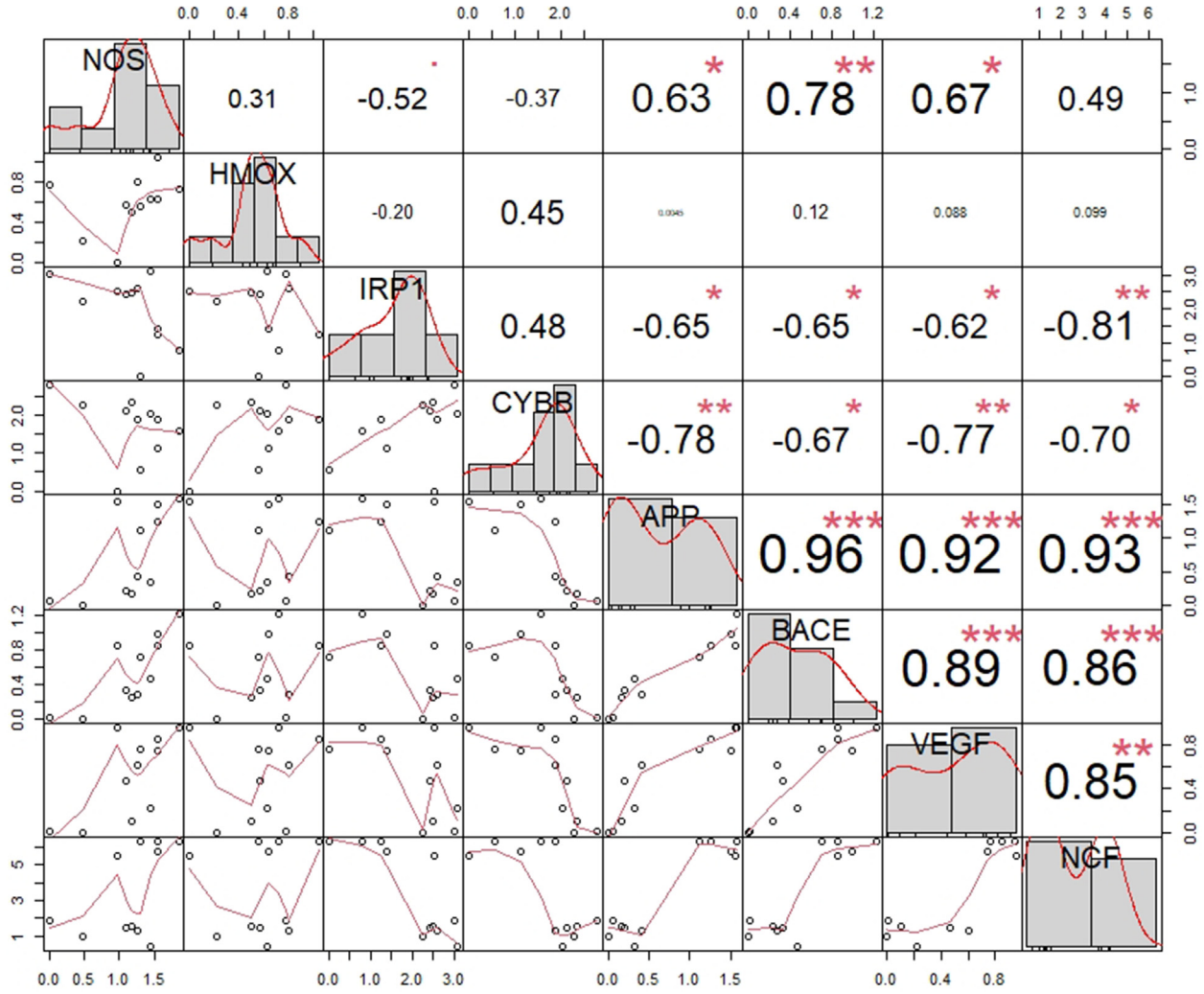

Figure 1. Scatter plot matrix showing the correlation coefficients between variables and the significance levels.

84.8% of variable cloud total variability is explained by the plane. This percentage is high and thus the first plane represents an important part of the data variability (Figure 3).

Biplot is one of the most informative graphical representations of a multivariate dataset (Chapman et al., 2002). The angle between vectors reflects how variables correlate with one another: a small angle implies a positive correlation, a large one suggests a negative correlation, and a 90° angle indicates no correlation between two characteristics (Gabriel, 1971). In the biplot graph (Figure 4) we can see that the Control and PCB groups are clustered on the negative values of the x-axis. The rest of the groups (Glutamate and PCB + Glutamate) are grouped in positive values of the x-axis. The Wilks test p-value indicates that categorical variable treatment explains the distance between the individuals (p-value = 0.00032). This means that the points of gravity for all treatment groups are well separated in the plane. It should be noted that the middle center of the PCB + Glutamate group shifts down the y-axis (2nd dimension) and differs from Glutamate and the rest of the groups.

In the first dimension (explaining 66.9% of total variation), it is visible that the *BACE*, *APP*, *VEGF*, and *NCF* display vectors along the same direction with a small angle, which means that they are strongly correlated. On the other side, *IRP1* and *CYBB* have vectors along the oppositive side with a negative correlation. In the second dimension (explaining 17.9 % of total variation) *HMOX* has a positive significant correlation ($p \leq 0.05$) according to the Factomainer's function dimdesc ("FactoMineR: Exploratory Multivariate Data Analysis with R″ n.d.).

According to the ascending hierarchical classification of individuals, the classification carried out on individuals reveals 4 groups (Tab. S4-Suppl). Cluster 1 formed by individuals from the Control group is characterized by low values for the variables *NOS*, *VEGF*, and *BACE* (the variables are ordered from the weakest). Cluster 2 (PCB) is made up of individuals who share low values for the *NCF* variable. Cluster 3 (PCB + Glutamate) is characterized by low values for the variables *HMOX* and *CYBB* (the variables are ordered from the weakest). And, Cluster 4

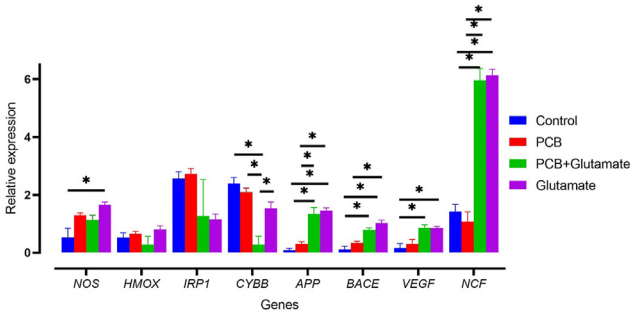

Figure 2. *NOS, HMOX, IRP1, CYBB, APP, BACE, VEGF*, and *NCF* mRNA expression levels. SH-SY5Y cells were stimulated or not with Glutamate 60 mM, PCB 0.1/0.01uM + Glutamate 60mM and PCB 0.1/0.01uM alone. Bars represent mean ± SEM (n = 3 experimental samples). *p < 0.05 by Tukey-Kramer posttest.

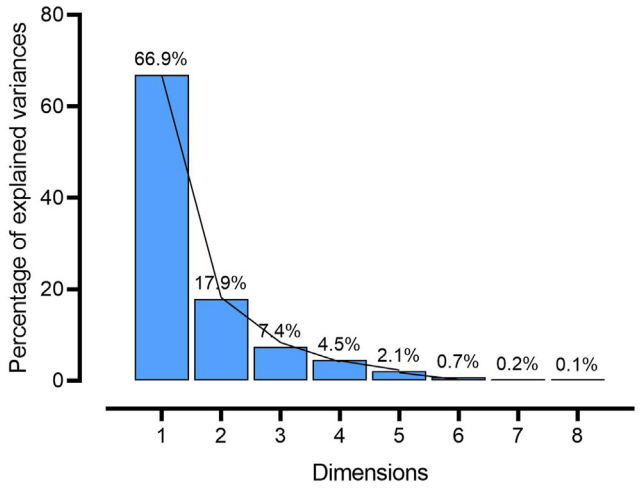

Figure 3. Decomposition of the total inertia. The first 2 factors are majors and express 84.8% of the data variability.

formed by individuals from the Glutamate group is characterized by high values for the variables *NCF*, *BACE*, *APP*, and *VEGF* (the variables are ordered from the strongest). And low values for the IRP1 variable.

Among all analyzed genes we would like to hallmark *CYBB* and *HMOX,* both detected by PCA as the most important variables in PCB + Glutamate group, which showed a strong correlation with the first and second dimensions, respectively. In the biplot diagram, it is observed that both gene vectors have an opposite direction to the group of samples of PCB + Glutamate, for this reason, the expression of both genes in this group is decreased. This analysis also corroborates the upregulation of *CYBB*, making *CYBB* an important therapeutic target of PCB for neurodegenerative diseases such as AD and stroke.

3.4. Differentially expressed genes in SH-SY5Y cells treated with PCB and subjected to medium-level glutamate injury

In this study, 60 mM is a relatively high concentration compared to other excitotoxic damage studies evaluated by our group (Fig. S3 Suppl) and references from other authors (Sun et al., 2010). For this reason, and taking into account that PCB downregulates *CYBB* and *HMOX-1* genes, we further evaluated the effect of PCB on the expression of other genes related to oxidative stress, cell death, and inflammation in the induced excitotoxic model by 40 mM glutamate.

In Figure 5, PCB regulates Glutamate effect on genes *HIF1A*, *SOD2*, *NFKB1*, *GPX1*, and *CAT*. In this group of cells damaged with Glutamate and treated with PCB, this molecule up-regulates the genes of the detoxifying enzymes *SOD2* and *CAT,* apoptosis related Bax and Bcl-2, the antioxidant gene *GPX1* and the transcription factor *NFBK1*. Of particular interest was PCB downregulation of the gene encoding *HIF1A* in this group of cells subjected to glutamate damage.

3.5. Effects of PCB in animal models of neurodegenerative diseases and cerebral ischemia

In Figure 6, pharmacological actions of PCB in the animal model of MS (EAE) referring to the clinical signs of animals treated with PCB was tested. Although without a significant difference between the groups ($p = 0.0899$, unpaired t test), it can be observed a clear tendency to reduction in the clinical severity of the disease promoted by the treatment with PCB.

In an EAE model (Figure 7), we evaluated the effect of PCB on pro-inflammatory cytokine levels in the brain of animals with EAE and treated with PCB. The results demonstrated a reduction in the levels of the pro-inflammatory cytokines IL-17, IFNgamma, and IL-6 in the brain of PCB-treated animals.

Finally, in a model of cerebral ischemia-induced by endothelin-1 (Figure 8), using immunohistochemical tools by electron microscopy, with the use of anti-CD11 antibodies to show macrophages markers of innate immune response and anti-cascape-3 antibody, marker apoptosis, we demonstrated preservation of macrophages/microglia as well as the myelin sheath, in animals treated with PCB.

4. Discussion

We investigated the effect of PCB in reverting the neurotoxicity insult provoked by Glutamate in SH-SY5Y cells. Using a set of genes we compared the expression in different groups of cells treated with PCB,

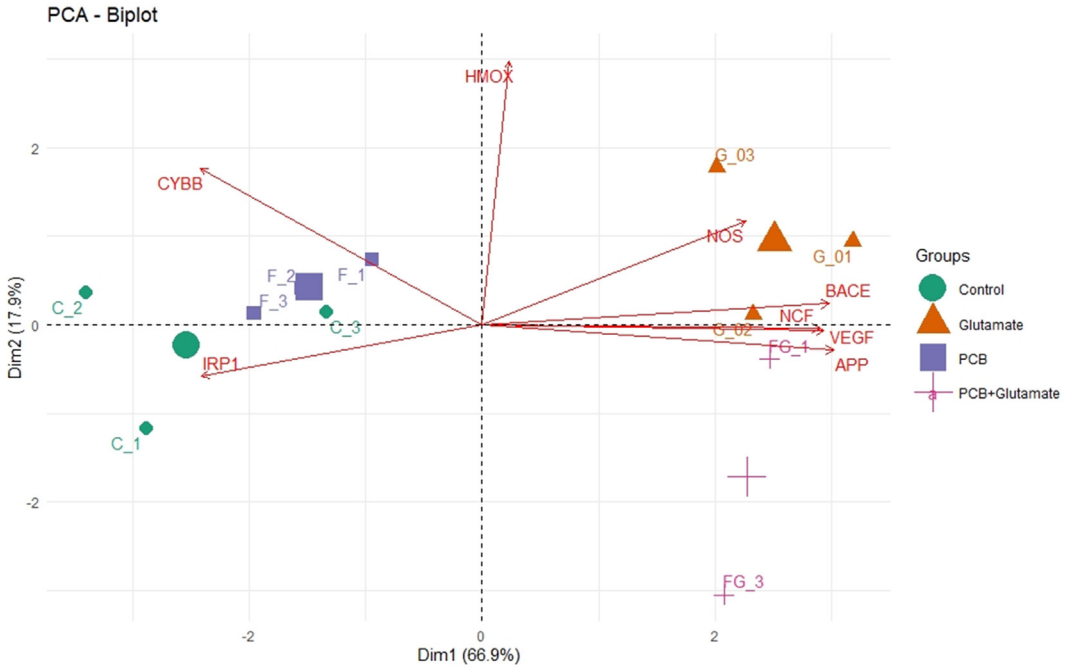

Figure 4. Biplots of a principal component analysis performed on the interaction between the factors gene and treatment.

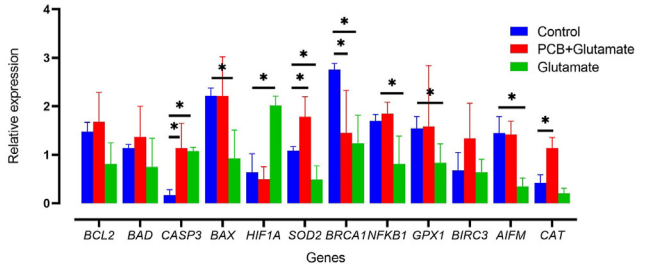

Figure 5. *BCL2, BAD, CASP3, BAX, HIF1A, SOD2, BRCA1, NFKB1, GPX1, BIRC3, AIFM1* and *CAT* mRNA expression levels. SH-SY5Y cells were stimulated or not with Glutamate (40 mM) or PCB(0.1/0.01uM) + Glutamate 40 mM. Bars represent mean ± SEM (n = 3 experimental samples). *p < 0.05 by Tukey-Kramer posttest.

Glutamate, Glutamate plus PCB, and Control non-treated cells. To achieve this purpose, we used the RT-qPCR technology. Data analysis using parametric ANOVA -Tukey Kramer and multivariate analysis of PCA to obtain evidence of the neuroprotective effect of PCB from the glutamate-induced excitotoxicity model in the SH-SY5Y cell line allowed to identify the relevant role of the genes.

We found a significant downregulation of *CYBB* as the major contributor to mitigate the Glutamate toxicity in SH-SY5Y using ANOVA. Meanwhile, using multivariate PCA two genes were identified as the most relevant in the PCB + Glutamate group: *CYBB* and *HMOX-1*. The *CYBB* gene encodes cytochrome b-245 protein, also known as p91-phox or NOX2, which forms part of an enzyme complex called NADPH oxidase (Rastogi et al., 2017). NOX plays an important role in some neurological disorders such as neurodegenerative diseases, including Multiple Sclerosis (MS) and Alzheimer's Disease (AD) ("*CYBB* Gene: MedlinePlus Genetics" n.d.). This enzyme converts oxygen into a toxic molecule radical anion superoxide. The main function of NADPH oxidases (NOX1-5) is to induce ROS. A disbalance in NOX-associated ROS regulation can result in promoting oxidative stress, aberrant signaling, and genomic instability (Nitti et al., 2018). Increased NOX activity is associated with the early expression of dementia, most likely as a result of increased ROS and subsequent oxidative stress. NOX also contributes to the pathogenesis of numerous inflammation-related peripheral diseases, such as atherosclerosis, diabetes, hypertension, ischemic stroke, and cardiovascular disease (Martínez et al., 2019).

PCB has been reported to inhibit various isoforms of NADPH oxidase in models of various diseases, for example, the expression of p22phox in hamsters fed an atherogenic diet (Riss et al., 2007); NOX4, p22phox, and p47phox in diabetic mice (Zheng et al., 2013), suggesting a cytoprotective action of PCB. Reduction of *CYBB* expression in cells subjected to treatment with PCB + Glutamate in comparison with the Control and Glutamate groups was evidenced here. This reduction in NOX2 expression may protect the cell from glutamate attack, probably by reducing ROS release and oxidative stress. This result is consistent with the findings of Marín-Prida et al., (2013) who demonstrated that PCB is neuroprotective in PC12 cells subjected to oxidative stress or excitotoxicity-induced alterations.

NOX additionally promotes the activation of inflammatory cytokines, including TGF-β, TNF-α, NF-kβ, IL-6, and IL-18, and VEGF (Laddha and Kulkarni, 2020). In our study, it was shown that PCB was able to reduce clinical signs and levels of pro-inflammatory cytokines such as IL-17, IFNg, and IL-6 in the brain of the EAE model, probably due to its anti-inflammatory effect linked to its antioxidant effect, as we have shown in previous reports from our team (Pentón-Rol and Cervantes-Llanos, 2018). A similar situation was found in this study regarding cerebral ischemia in which beneficial pharmacological actions of PCB with respect to behavioral tests and reduction of cerebral infarct volume was shown in a study of our group (Pavón-Fuentes et al., 2020).

Another interesting result of this study was the downregulation of the *HMOX-1* gene by PCB. *HMOX-1* encodes for the heme oxygenase 1 that mediates the catabolism of heme groups into carbon monoxide, biliverdin, and ferrous iron. We observed a reduction in the expression of *HMOX-1* in the group of PCB + Glutamate compared to Glutamate. There is also evidence that its up-regulation is associated with the late phase of neurodegeneration and has been proposed as a biomarker of AD (Schipper, 2007). According to Gupta et al. induction of the glial *HMOX-1* gene contributes to pathological brain iron deposition, intracellular oxidative damage, and bioenergetic failure in AD and other human CNS disorders. According to Gupta et al. *HMOX-1* gene can contribute to some disorders such as iron deposition in the brain, intracellular oxidative damage, and bioenergetic failure in AD. Therefore, downregulation of

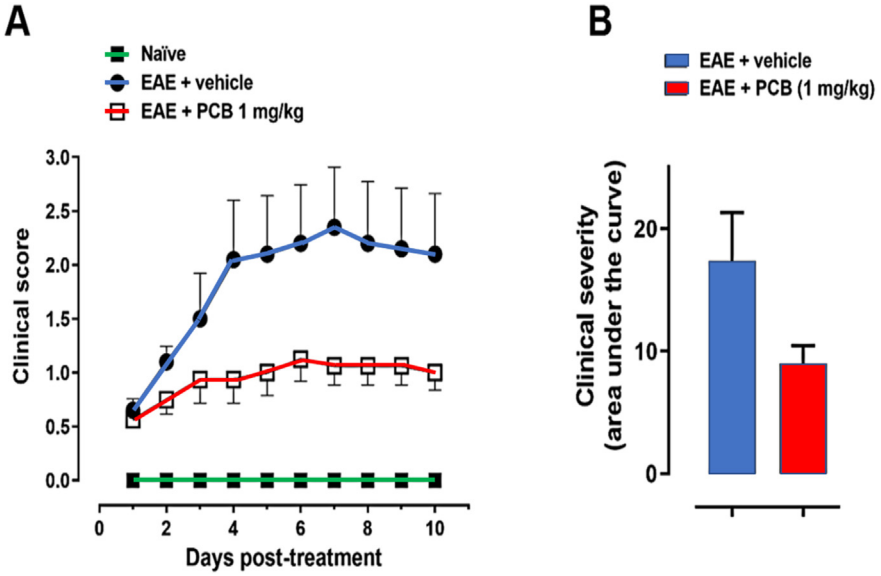

Figure 6. Clinical assessment of the oral administration of PCB in EAE mice. Graphic indicates the Clinical Score (A) and the disease severity (B) during the study period. C57BL/6 female mice immunized with MOG $_{35–55}$ were treated daily with PCB at 1 mg/kg orally starting on the onset of symptoms until the end of the study (day 28). Animals were scored each day using a clinical signs scale from 0 (no disease) to 5 (death). Data are expressed as the mean ± S.E.M (n = 8–10 per group).

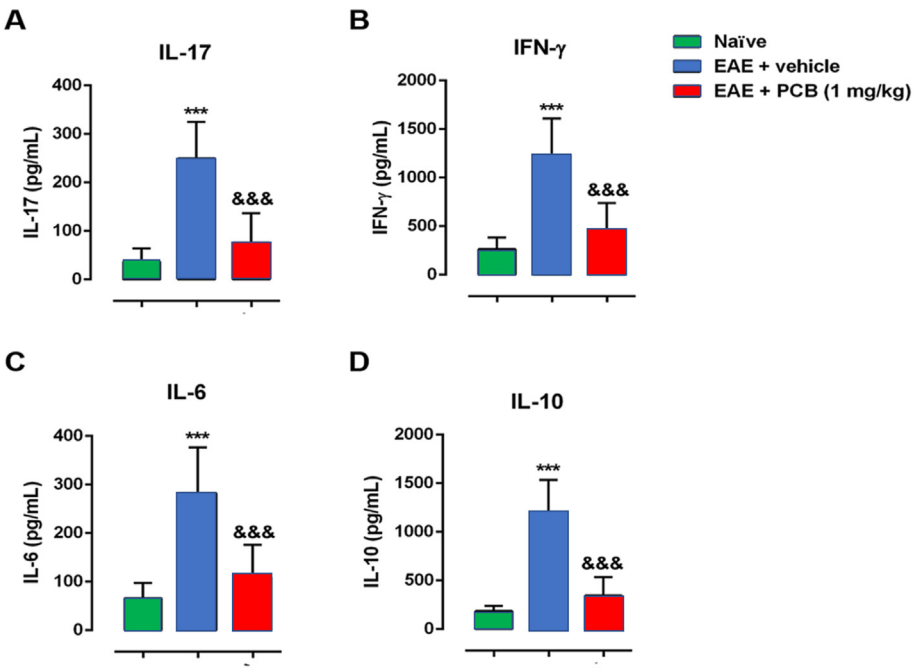

Figure 7. Effects of oral treatment with PCB on proinflammatory cytokine levels in EAE mice. C57BL/6 female mice immunized with MOG $_{35–55}$ were treated daily with PBS (vehicle) or PCB 1 mg/kg orally started at disease onset, when the mice got sick until the end of the study (day 28). At this time point, the cytokines levels were assessed by ELISA from brain samples. Data are expressed as mean ± S.E.M. (n = 8–10 per group). Ampersand (&) and asterisk (*) indicate significant differences with non-immunized naïve and vehicle-treated EAE rats, respectively.

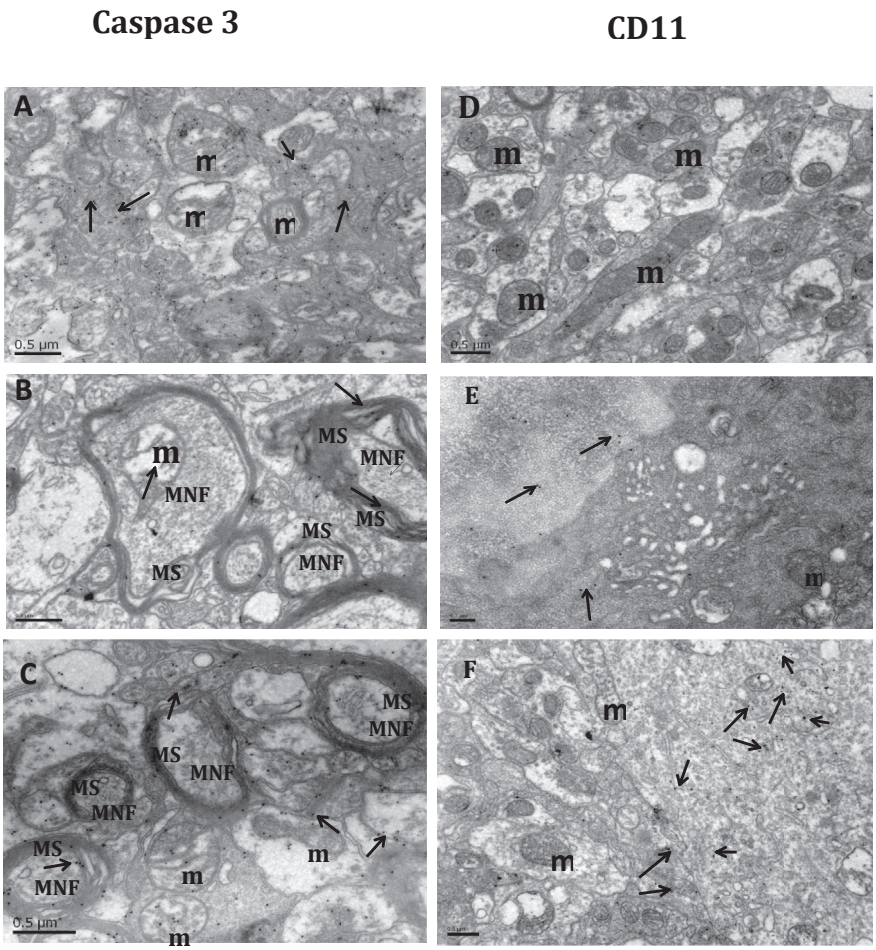

Figure 8. Phycocyanobilin effects on caspase 3 and CD11 expression levels assessed by immunoelectron microscopy at the cerebral cortex 24 h after ischemia/reperfusion (I/R). Representative photographs of sham (**A, D**), I/R + vehicle (**B, E**) and I/R + PCB 200 µg/kg (**C,F**) (n = 5 each group). Arrows indicate the immunodetection of each marker. Bar: 0.5 µm. Abbreviations: **m**= mitochondria; **MS**= Myelin Sheet; **MNF**= Myelinic Nerve Fiber.

glial *HMOX-1* hyperactivity could be considered an effective therapeutic intervention in AD and other neurodegenerative disorders. For the first time, they demonstrated that suppression of *HMOX-1* activity ameliorates neuroinflammatory responses and cognitive deficits in a mouse model of AD (Gupta et al., 2014), supporting the benefit of downregulation of this gene by PCB.

Interestingly, another annotation that we can make from the biplot analysis is related to *NOS1*. In the study, we can see that the Glutamate group is characterized by a high expression of *NOS1*, while the PCB + Glutamate group showed a lower expression compared to Glutamate. This reduction in the expression of *NOS1* by the action of PCB leads to the hypothesis that PCB can modulate NO to neuroprotective physiological levels in SH-SY5Y cells.

From the downregulation of the *CYBB* gene by PCB, in our study, we evaluated other genes related to enzymes with a detoxification role of the organism, *SOD1*, *CAT,* and *GPX*. The results demonstrated that there was an upregulation by PCB of the genes encoding both enzymes, perhaps as a homeostatic mechanism for the elimination of the superoxide radical.

One of the most interesting results of the study was the downregulation of the *HIF1A* gene. The *HIF1A* gene has been linked to the response to hypoxia. Its function may involve both adaptations to present stress conditions. The mechanism by which the intermittent hypoxia (IH) can impair hippocampal synaptic plasticity and spatial memory has been associated with redox state changes by *HIF1A*. Moreover, Arias-Cavieres et al., 2020 reported that IH-dependent HIF1a signaling can induce the expression of the NADPH oxidase 4 (NOX4). In this sense, a downregulation of the *HIF1A* gene by PCB could reduce the generation of ROS, also directed by the downregulation of *NOX2*.

Previously, oxidative damage was observed in our studies (Marín-Prida et al., 2013) in glutamate-treated PC12 cells, all of which was relieved by PCB. In this study, SY-SY5Y cells were treated with Glutamate and Glutamate plus PCB and there was upregulation of the *BACE* and *APP* genes in both groups. PCB treatment was unable to down-regulate the effect produced by Glutamate on both genes. We postulate that the glutamate concentration used was too high to be counteracted by PCB or perhaps a higher concentration of PCB is necessary to achieve an effect on these molecules. In this sense, reports show that C-Phycocyanin (in which PCB is included) reduced the protein levels of *APP* and *BACE* (Koh et al., 2018).

Cell death and neurodegenerative conditions have been linked to oxidative stress and imbalance between the generation of free radicals and antioxidant defenses (E. Radi et al., 2014). In this study, PCB up-regulated 2 of the genes evaluated *Bax* and *BCL2*. However, immunohistochemical experiments with anti-Caspase 3 in a model of cerebral ischemia-induced by endothelin 1 evidenced the positive inducing effect of Caspase 3 by PCB. In our study, PCB increased immunoidentification with anti-caspase-3, which is in line with the results obtained in which a silent RNA for caspase-3 was only marginally effective in suppressing growth inhibition and cell death indicating that the mechanism is complex and that other cellular processes in addition to apoptosis may also contribute to the anti-apoptotic effect of PCB (Liao et al., 2016). The increase in the immuno-identification of macrophages with anti-CD11 by PCB was detected, supporting that macrophages are fundamental for the regeneration process of the central nervous system and remyelination, highlighting the pro-regenerative role of the innate immune system and the effect of PCB, which is in agreement with the works of our group that refer to the effect of PCB on myelin (Pentón-Rol et al. 2018).

An exacerbated pro-inflammatory response may be due to the activation of the oxidative stress machinery combined with factors that regulate innate immunity such as NF-kB. In this sense, in our study we aimed to evaluate the "*in vivo*" effect of PCB in animal models with the aim of translating the in vitro results, so far obtained in the Glutamate-induced excitotoxicity model in SH-SY5Y cells, to demonstrate the in vivo effect of PCB in animal models in which oxidative stress, inflammation, and immune dysfunction play a predominant role in its pathogenic mechanism.

NF-κB is a pleiotropic transcription factor that plays a central role in the innate and acquired immune response, inducing the expression of genes encoding proinflammatory cytokines, chemokines, adhesion molecules, and regulators of apoptosis. A pro/antioxidant imbalance contributes to the pathologic process of many human diseases, and ROS depending on the cell context can induce or repress NF-κB signaling (Lingappan, 2018). The positive regulation by PCB (in the reverse direction of Glutamate) of the expression of the *NFKB1* gene points to the need for exquisite regulatory mechanisms.

Finally, our "*in vitro*" and "*in vivo*" results indicate that PCB has achieved marked protective effects in cells and in rodent animal models of ischemic stroke and multiple sclerosis, and suggests that PCB could also be protective against Alzheimer's disease and its effective anti-inflammatory, in the recent COVID-19 pandemic reducing the "cytokine storm."

5. Conclusions

In the present work, we study how, from the optimization of the qPCR data analysis concerning a biological hypothesis, the results can be validated and redirected. Initially, genes relevant to the biological effect of PCB were studied by comparing them with qPCR data analysis methodologies: ANOVA and PCA. The biological relevance of the downregulation by PCB of the *CYBB* and, *HMOX-1* genes was fundamentally identified, and from this result a rational design was carried out in the same model of excitotoxicity induced by Glutamate, of other main genes, obtaining an up-regulation of *SOD1* and *CAT* (oxidative stress), *BCL2*, *Bax* (apoptosis), transcriptional factors *NFkB1* (inflammation) and the downregulation of the *HIF1A* gene (hypoxia). The results obtained "*in vitro*" on the modulation of genes by PCB were transferred to the evaluation of the "*in vivo*" effect of PCB in 2 animal models of MS and stroke in whose pathogenesis, oxidative stress, and inflammation play a relevant role. The results in the MS model showed a reduction by PCB of pro-inflammatory cytokines in the brain of animals and in the animal model of stroke the induction by PCB of the innate immune response and apoptosis. In summary, our results range from the effect of PCB on gene modulation to therapy in animal models.

Declarations

Author contribution statement

Daniel Palenzuela Gardón, Majel Cervantes-Llanos: Conceived and designed the experiments; Performed the experiments; Analyzed and interpreted the data; Contributed reagents, materials, analysis tools or data; Wrote the paper.

Beatriz Piniella Matamoros, Hanlet Camacho Rodríguez, Chan-yuan Tan, Laura de la Caridad Bakos Ruiz, Tamara Díaz Argudin: Performed the experiments; Analyzed and interpreted the data.

Javier Marín –Prida, Viviana Falcón-Cama, Nancy Pavón-Fuentes, Jessica Gómez Lemus: Analyzed and interpreted the data; Contributed reagents, materials, analysis tools or data; Wrote the paper.

Gillian Martínez Donato, Yasser Perera, Ke Yang, Giselle Pentón-Rol: Conceived and designed the experiments; Analyzed and interpreted the data; Wrote the paper.

Funding statement

This work was supported by "Hunan Provincial Base for Scientific and Technological Innovation Cooperation", China, grant number 2019CB1012.

Data availability statement

Data included in article/supplementary material/referenced in article.

Declaration of interests statement

The authors declare no conflict of interest.

Additional information

Supplementary data to this article can be found online at https://doi.org/10.1016/j.heliyon.2022.e09769.

Acknowledgements

We are grateful to Dr Leonora Gonzalez Mesa for her support in cell culture experiments.

References

Anesthesia and Analgesia in Laboratory Animals - 2nd Edition. n.d. Accessed September 10, 2021. https://www.elsevier.com/books/anesthesia-and-analgesia-in-laboratory-animals/fish/978-0-12-373898-1.

Bae, Yun Soo, Oh, Hyunjin, Goo Rhee, Sue, Yoo, Young Do, 2011. Regulation of reactive oxygen species generation in cell signaling. Mol. Cell. 32 (6), 491–509.

Chapman, Scott, Peer Schenk, Kazan, Kemal, Manners, John, 2002. Using biplots to interpret gene expression patterns in plants. Bioinformatics 18 (1), 202–204.

Chen, Shi-Yi, Feng, Zhe, Yi, Xiaolian, 2017. A general introduction to adjustment for multiple comparisons. J. Thorac. Dis. 9 (6), 1725–1729.

Chen, Xueping, Guo, Chunyan, Kong, Jiming, 2012. Oxidative stress in neurodegenerative diseases. Neural Regeneration Research 7 (5), 376–385.

Chengalvala, Murty V., Chennathukuzhi, Vargheese M., Johnston, Daniel S., E Stevis, Panayiotis, Kopf, Gregory S., 2007. Gene expression profiling and its practice in drug development. Curr. Genom. 8 (4), 262–270.

CYBB Gene: MedlinePlus Genetics. n.d. Accessed July 22, 2021. https://medlineplus.gov/genetics/gene/cybb/.

FactoMineR. Exploratory multivariate data analysis with R. n.d. Accessed August 18, 2021. http://factominer.free.fr/.

Fernández-Rojas, Berenice, Hernández-Juárez, Jesús, Pedraza-Chaverri, José, 2014. Nutraceutical properties of phycocyanin. J. Funct.Foods 11 (November), 375–392.

Gabriel, K.R., 1971. The biplot graphic display of matrices with application to principal component analysis on JSTOR. Biometrika 58 (3), 433, 367.

Gupta, Ajay, Lacoste, Baptiste, Pistell, Paul J., Pistel, Paul J., Ingram, Donald K., Hamel, Edith, Moulay, A., Alaoui-Jamali, et al., 2014. Neurotherapeutic effects of novel HO-1 inhibitors in vitro and in a transgenic mouse model of alzheimer's disease. J. Neurochem. 131 (6), 778–790.

Henrik, Laurell, Iacovoni, Jason S., 2012. Correction of RT–QPCR data for genomic DNA-derived signals with ValidPrime. In: Nucleic Acids Research Advance Access, 6. https://www.ncbi.nlm.nih.gov/pmc/articles/PMC3326333/.

Jolliffe, Ian T., Jorge, Cadima., 2016. Principal component analysis: a review and recent developments. Phil. Trans. Math. Phys. Eng. Sci. 374 (2065), 20150202.

Koh, Eun-Jeong, Kim, Kui-Jin, Jia, Choi, Kang, Do-Hyung, Lee, Boo-Yong, 2018. Spirulina maxima extract prevents cell death through BDNF activation against amyloid beta 1-42 (Aβ1-42) induced neurotoxicity in PC12 cells. Neurosci. Lett. 673 (April), 33–38.

Laddha, Ankit P., Kulkarni, Yogesh A., 2020. NADPH oxidase: a membrane-bound enzyme and its inhibitors in diabetic complications. Eur. J. Pharmacol. 881 (August), 173206.

Lech, Maciej, Anders, Hans-Joachim, 2014. Expression profiling by real-time quantitative polymerase chain reaction (RT-QPCR). Methods Mol. Biol. 1169, 133–142.

Liao, Gaoyong, Gao, Bing, Gao, Yingnv, Yang, Xuegan, Cheng, Xiaodong, Ou, Yu, 2016. Phycocyanin inhibits tumorigenic potential of pancreatic cancer cells: role of apoptosis and autophagy. Sci. Rep. 6 (October), 34564.

Lingappan, Krithika, 2018. NF-KB in oxidative stress. Current Opinion in Toxicology 7 (February), 81–86.

Marín-Prida, Javier, Pavón-Fuentes, Nancy, Llópiz-Arzuaga, Alexey, Julio, R., Fernández-Massó, Delgado-Roche, Liván, Mendoza-Marí, Yssel, Pedroso Santana, Seydi, et al., 2013. Phycocyanobilin promotes PC12 cell survival and modulates immune and inflammatory genes and oxidative stress markers in acute cerebral hypoperfusion in rats. Toxicol. Appl. Pharmacol. 272 (1), 49–60.

Martindale, Jennifer L., Holbrook, Nikki J., 2002. Cellular response to oxidative stress: signaling for suicide and survival. J. Cell. Physiol. 192 (1), 1–15.

Martínez, María-Aránzazu, Rodríguez, José-Luis, Lopez-Torres, Bernardo, Martínez, Marta, María-Rosa Martínez-Larrañaga, Anadón, Arturo, Ares, Irma, 2019. Oxidative stress and related gene expression effects of cyfluthrin in human neuroblastoma SH-SY5Y cells: protective effect of melatonin. Environ. Res. 177 (October), 108579.

Nitti, Mariapaola, Piras, Sabrina, Brondolo, Lorenzo, Maria Marinari, Umberto, Pronzato, Maria Adelaide, Lisa Furfaro, Anna, 2018. Heme oxygenase 1 in the nervous system: does it favor neuronal cell survival or induce neurodegeneration? Int. J. Mol. Sci. 19 (8), 2260.

Padyana, A.K., Bhat, V.B., Madyastha, K.M., Rajashankar, K.R., Ramakumar, S., 2001. Crystal structure of a light-harvesting protein C-phycocyanin from Spirulina platensis. Biochem. Biophys. Res. Commun. 282 (4), 893–898.

Pavón-Fuentes, Nancy, Marín-Prida, Javier, Llópiz-Arzuaga, Alexey, Falcón-Cama, Viviana, Campos-Mojena, Rosario, Cervantes-Llanos, Majel, Piniella-Matamoros, Beatriz, Pentón-Arias, Eduardo, Pentón-Rol, Giselle, 2020. Phycocyanobilin reduces brain injury after endothelin-1- induced focal cerebral ischaemia. Clin. Exp. Pharmacol. Physiol. 47 (3), 383–392.

Pentón-Rol, Giselle, Cervantes-Llanos, Majel, 2018. Report on the symposium 'molecular mechanisms involved in neurodegeneration. Behav. Sci. 8 (1).

Pentón-Rol, Giselle, Marín-Prida, Javier, Falcón-Cama, Viviana, 2018. C-phycocyanin and Phycocyanobilin as remyelination therapies for enhancing recovery in multiple sclerosis and ischemic stroke: a preclinical perspective. Behav. Sci. 8 (1).

Pentón-Rol, Giselle, Marín-Prida, Javier, McCarty, Mark F., 2021. C-Phycocyanin-Derived Phycocyanobilin as a potential nutraceutical approach for major neurodegenerative disorders and COVID-19-induced damage to the nervous system. Curr. Neuropharmacol. April.

PrimePCR Pathways. n.d. Accessed December 22, 2021. https://commerce.bio-rad.com/en-usoprime-pcrsassays/panhway/primepcr-patdways#tab-5.

Radi, Elena, Formichi, Patrizia, Battisti, Carla, Federico, Antonio, 2014. Apoptosis and Oxidative Stress in Neurodegenerative Diseases. J. Alzheim. Dis.: JAD 42 (Suppl 3), S125–152.

Radi, Rafael, 2018. Oxygen radicals, nitric oxide, and peroxynitrite: redox pathways in molecular medicine. Proc. Natl. Acad. Sci. U.S.A. 115 (23), 5839–5848.

Rastogi, Radhika, Geng, Xiaokun, Li, Fengwu, Ding, Yuchuan, 2017. NOX activation by subunit interaction and underlying mechanisms in disease. Front. Cell. Neurosci. 10 (January), 301.

Riss, Jérome, Kelly, Décordé, Thibault Sutra, Delage, Martine, Baccou, Jean-Claude, Jouy, Nicolas, Brune, Jean-Pierre, Oréal, Henri, Cristol, Jean-Paul, Rouanet, Jean-Max, 2007. Phycobiliprotein C-phycocyanin from Spirulina platensis is powerfully responsible for reducing oxidative stress and NADPH oxidase expression induced by an atherogenic diet in hamsters. J. Agric. Food Chem. 55 (19), 7962–7967.

Rodriguez-Esteban, Raul, Jiang, Xiaoyu, 2017. Differential gene expression in disease: a comparison between high-throughput studies and the literature. BMC Med. Genom. 10 (October), 59.

Schipper, Hyman M., 2007. Biomarker potential of heme oxygenase-1 in alzheimer's disease and mild cognitive impairment. Biomarkers Med. 1 (3), 375–385.

Spurr, Arthur R., 1969. A low-viscosity epoxy resin embedding medium for electron microscopy. J. Ultra. Res. 26 (1), 31–43.

Sun, Zhong-Wei, Zhang, Lan, Zhu, Shu-Jia, Chen, Wen-Chun, Mei, Bing, 2010. Excitotoxicity effects of glutamate on human neuroblastoma SH-SY5Y cells via oxidative damage. Neurosci. Bull. 26 (1), 8–16.

Xie, Hong-rong, Hu, Lin-sen, Li, Guo-yi, 2010. SH-SY5Y human neuroblastoma cell line:in vitrocell model of dopaminergic neurons in Parkinson's disease. Chinese Med J 123 (8), 1086–1092.

Zheng, Jing, Inoguchi, Toyoshi, Sasaki, Shuji, Maeda, Yasutaka, McCarty, Mark F., Fujii, Masakazu, Ikeda, Noriko, Kobayashi, Kunihisa, Sonoda, Noriyuki, Takayanagi, Ryoichi, 2013. Phycocyanin and Phycocyanobilin from Spirulina platensis protect against diabetic nephropathy by inhibiting oxidative stress. Am. J. Physiol. Regul. Integr. Comp. Physiol. 304 (2), R110–R120.